Manuscript prepared for Atmos. Chem. Phys.
with version 2014/07/29 7.12 Copernicus papers of the LaTeX class copernicus.cls.
Date: 28 September 2015

A qualitative comparison of secondary organic aerosol (SOA) yields and composition from ozonolysis of monoterpenes at varying concentrations of NO_2

D. C. Draper[1,*], D. K. Farmer[2], Y. Desyaterik[3], and J. L. Fry[1]

[1]Department of Chemistry, Reed College, Portland, OR, USA
[2]Department of Chemistry, Colorado State University, Fort Collins, CO, USA
[3]Department of Atmospheric Science, Colorado State University, Fort Collins, CO, USA
[*]current address: Department of Chemistry, University of California Irvine, Irvine, CA, USA

Correspondence to: J. L. Fry, fry@reed.edu

Abstract.

The effect of NO_2 on secondary organic aerosol (SOA) formation from ozonolysis of α-pinene, β-pinene, Δ^3-carene, and limonene was investigated using a dark flow-through reaction chamber. SOA mass yields were calculated for each monoterpene from ozonolysis with varying NO_2 concentrations. Kinetics modeling of the first generation gas-phase chemistry suggests that differences in observed aerosol yields for different NO_2 concentrations are consistent with NO_3 formation and subsequent competition between O_3 and NO_3 to oxidize each monoterpene. α-pinene was the only monoterpene studied that showed a systematic decrease in both aerosol number concentration and mass concentration with increasing [NO_2]. β-pinene and Δ^3-carene produced fewer particles at higher [NO_2], but both retained moderate mass yields. Limonene exhibited both higher number concentrations and greater mass concentrations at higher [NO_2]. SOA from each experiment was collected and analyzed by HPLC-ESI-MS, enabling comparisons between product distributions for each system. In general, the systems influenced by NO_3 oxidation contained more high molecular weight products (MW > 400 amu), suggesting the importance of oligomerization mechanisms in NO_3-initiated SOA formation. α-pinene, which showed anomalously low aerosol mass yields in the presence of NO_2, showed no increase in these oligomer peaks, suggesting that lack of oligomer formation is a likely cause of α-pinene's near 0 % yields with NO_3. Through direct comparisons of mixed-oxidant systems, this work suggests that NO_3 is likely to dominate nighttime oxidation pathways in most regions with both biogenic and anthropogenic influences. Therefore, accurately constraining SOA yields from NO_3 oxidation, which vary substantially with the VOC precursor, is essential in predicting nighttime aerosol production.

1 Introduction

Secondary organic aerosol (SOA) forms in the atmosphere from oxidized volatile organic compounds (VOCs) that are of low enough volatility to be able to partition into the condensed phase. Aerosol directly affects Earth's radiative balance and also contributes to cloud formation, both of which have important climate forcing implications (IPCC, 2013). Aerosol is responsible for regional haze, and has been shown to cause adverse cardiopulmonary health effects (Pope III et al., 1995; Davidson et al., 2005). SOA constitutes a large fraction of the total aerosol budget, but it is still poorly constrained in global chemical transport models, which underpredict ambient aerosol concentrations by one to two orders of magnitude (Heald et al., 2005, 2011). These models use laboratory-derived parameters, but uncertainty in precursors, detailed mechanisms, and mechanistic differences between chamber simulations and the real atmosphere result in the vast discrepancies between models and observations (Kroll and Seinfeld, 2008; Hallquist et al., 2009).

Nearly 90% of the non-methane VOCs emitted globally are biogenic in origin, so it should follow that a large fraction of the uncertainty in model predictions of the SOA budget comes from uncertainty in how biogenic VOCs (BVOCs) form aerosol (Guenther et al., 1995; Middleton, 1995). Different plant species emit different types and ratios of BVOCs, so the specific distribution of BVOCs emitted to the atmosphere is dependent on unique mixtures of vegetation and thus varies a great deal regionally. Monoterpenes are one such class of BVOC that is both widely emitted and has been shown in the laboratory to efficiently produce SOA (Goldstein and Galbally, 2007; Sakulyanontvittaya et al., 2008; Griffin et al., 1999; Hallquist et al., 1999; Ng et al., 2006; Ehn et al., 2014; Hoyle et al., 2011). On average in the United States, α-pinene is the most dominant monoterpene emission, but β-pinene, Δ^3-carene, and limonene (Figure 1) are also prevalent and are emitted equally or more than α-pinene in some regions (Geron et al., 2000).

While most VOCs are biogenic, the majority of atmospheric oxidants are anthropogenically sourced, and thus human activity is highly influential on SOA production (Carlton et al., 2010; Hoyle et al., 2011; Xu et al., 2015). At night, most VOC oxidation in the troposphere occurs by way of either photolabile nitrate radical (NO_3) or longer-lived ozone (O_3), which is photochemically produced but is not rapidly and completely consumed at sundown as is the hydroxyl radical (OH). The formation of both of these tropospheric oxidants requires NO_2, nearly 90% of which in the US (64% globally) is estimated to come from anthropogenic sources (Reis et al., 2009). Organonitrates have been observed in ambient nighttime aerosol during multiple field studies (Fry et al., 2013; Rollins et al., 2012; Xu et al., 2015), consistent with NO_3 oxidation, and NO_3 initiated production of aerosol organonitrates may even compete with photolysis of NO_3 during the day in some regions with high BVOC emissions (Ayres et al., 2015). These observations are consistent with several laboratory studies that have found moderate to high aerosol yields from NO_3 oxidation (Griffin et al., 1999; Hallquist et al., 1999; Fry et al., 2009, 2011, 2014; Spittler et al., 2006; Moldanova and Ljungström,

2000; Boyd et al., 2015), but this body of literature is comparatively small relative to OH and O_3 oxidation studies.

Most chamber studies of NO_3-derived SOA generate NO_3 through the thermal dissociation of N_2O_5 in order to minimize the complexity caused by introducing a second oxidant (Griffin et al., 1999; Hallquist et al., 1999; Fry et al., 2014). Fewer studies have been done using the atmospherically more relevant conditions of introducing both O_3 and NO_2 into the chamber to mimic this full range of nighttime oxidation chemistry (Perraud et al., 2012; Presto et al., 2005; Boyd et al., 2015). Perraud et al. (2012) and Presto et al. (2005) both studied the effects of a range of NO_2 concentrations on dark ozonolysis of α-pinene, and both observed that increased [NO_2] suppresses aerosol formation. To our knowledge, NO_2 effects on dark ozonolysis have not been systematically assessed for any other monoterpenes. Ozonolysis of α-pinene has been previously observed to have high (14-67%) aerosol yields (Hoffmann et al., 1997; Ng et al., 2006) but strikingly low (0-16%) SOA yields with NO_3 (Hallquist et al., 1999; Fry et al., 2014; Spittler et al., 2006). The observed aerosol suppression in the O_3 + NO_2 system is consistent with the increased contribution of NO_3 at higher [NO_2]. However, α-pinene is the only monoterpene that has been observed to have such drastic SOA yield discrepancies between the two oxidants (Ng et al., 2006; Yu et al., 1999; Hallquist et al., 1999; Fry et al., 2014), so it may not be reasonable to assume NO_2 has the same effect on other monoterpenes.

Here we focus on the four most prevalently emitted monoterpenes in the US: α-pinene, β-pinene, Δ^3-carene, and limonene. Table 1 shows rate constants for NO_3 formation from NO_2 + O_3 as well as each of the nighttime oxidants with the monoterpenes used in this study. It is evident that the rates of O_3 loss to NO_3 production and BVOC oxidation are comparable when [NO_2] and [BVOC] are similar. Even considering its smaller ambient concentrations, NO_3 oxidation is often much faster than O_3 oxidation, so it follows that NO_3 oxidation should provide an important contribution to nighttime aerosol formation in regions that are both biogenically- and anthropogenically-influenced. This work seeks to characterize the role of each competing nighttime oxidant over this broader range of monoterpenes and the influence of each on SOA formation.

2 Methods

Unseeded SOA formation experiments were performed in a darkened ~400 L PFA film chamber, shown in Figure 2, run in flow-through mode with precursors added continuously, giving a residence time of approximately 90 minutes. The set of experiments described in Table 2 measured the aerosol production from a single monoterpene oxidized by O_3 with varying concentrations of NO_2 added. In order to make comparisons across both the range of monoterpenes and the range of [NO_2], the monoterpene source and O_3 source concentrations were kept as constant as possible throughout the full study, allowing only the identity of the BVOC and the concentration of NO_2 to vary. While

precursor concentrations used in this study are all quite high and thus absolute observed aerosol yields are likely not atmospherically relevant due to high mass loadings and unrealistic radical fates, the ratios of $[O_3]$:$[NO_2]$ ranging from 1:0.5 to 1:4 are representative of ratios observable in the atmosphere from relatively clean sites (O_3 dominated) to heavily polluted sites (NO_2 dominated). Similarly, $[NO_2]$:[BVOC] ranging from approximately 1:1 to 2:1 is reasonable for relatively clean to relatively polluted sites, making comparisons between these conditions informative to aerosol formation in the real atmosphere.

O_3 (and NO_2, when applicable) were introduced into the chamber first and allowed to reach steady state prior to initiation of SOA formation by BVOC injection. O_3 was generated by flowing zero air (Sabio Model 1001 compressed zero air generator) through a flask containing a Pen-Ray Hg lamp (primary energy at 254 nm) and was continuously measured from the outlet of the chamber using a Dasibi Model 1003-AH O_3 monitor. NO_2 was introduced from a calibrated cylinder (Air Liquide, 0.3% by volume in N_2), and monitored using a Thermo Model 17i chemiluminescence NO_x/NH_3 analyzer. Chemiluminescence NO_x analyzers are sensitive to any species that is converted to NO in the 350 °C Mb converter responsible for converting NO_2 to NO (Winer et al., 1974; Grosjean and Harrison, 1985). Some of these additional species include N_2O_5, peroxy-nitrates (PNs), and alkyl-nitrates (ANs). At the high concentrations used in this study, these NO_y contributions were significant. Kinetics modeling of the oxidant stabilization period (described in the supplemental information), corroborated by a characterization of oxidant stabilization using chemiluminescence NO_x analyzers and a cavity ringdown spectrometer sensitive only to NO_2, indicates that we detected N_2O_5 with approximately unit efficiency in the NO_2 channel of the Thermo NO_x analyzer. The sensitivity of this NO_x analyzer to PNs and ANs, which would have formed following BVOC addition, was not calibrated, but is expected to be near unity based on previous studies (Winer et al., 1974; Grosjean and Harrison, 1985). Modeling only the oxidant stabilization period, where NO_2 and N_2O_5 were likely the only species detected in the NO_2 channel, provided the initial NO_2 concentrations shown in Table 2.

Once the oxidants stabilized, BVOC was introduced by flowing zero air over a small, cooled liquid sample of the target BVOC ((1R)-(+)-alpha-Pinene, TCI America, >95.0%; (-)-beta-Pinene, TCI America, >94%; (+)-3-Carene, TCI America, >90.0%; (R)-(+)-Limonene, Aldrich, >97%). The chiller temperature was held constant (± 0.3 °C) during a single experiment, and ranged from -27 to -21 °C for the different monoterpenes, based on the temperature-dependent vapor pressure that is calculated to give a mixing ratio of approximately 100 ppm in the source flask (Figure S.3) (Haynes et al., 2012). Since vapor pressure data was unavailable for Δ^3-carene, it was estimated to reach the temperature-dependent vapor pressure at -25 °C – between α-pinene and β-pinene target temperatures – due to structural similarities. Online BVOC measurements were not available, but reacted BVOC was calculated from the observed decay of the oxidant in the kinetics model for each exper-

iment. Methodology and uncertainties of this approach are described further in section 3.2 and the supplemental information.

Two methods were employed to measure the resulting aerosol loading and composition. Particle size distributions between 20 and 800 nm were measured at 85 s time resolution with a Scanning Electrical Mobility Sizer (SEMS; BMI Model 2002) consisting of a differential mobility analyzer (BMI Model 2000C) coupled to a Water Condensation Particle Counter (TSI Model 3781). Size-dependent aerosol loss rates to the chamber walls were characterized and used to correct size distributions to reflect the total aerosol number and volume concentrations produced in each experiment (McMurry and Grosjean, 1985; VanReken et al., 2006; Fry et al., 2014). This methodology is described in further detail in the supplemental information. Aerosol samples from each experiment were collected onto filters (47 mm quartz fiber). Each filter was extracted by sonication in 3:1 deionized water:acetonitrile to minimize solvent reactions with analyte compounds (Bateman et al., 2008), and the resulting extract was analyzed offline by High Performance Liquid Chromatography – Electrospray Ionization – Mass Spectrometry (HPLC-ESI-MS).

Due to its relatively soft ionization source and thus minimal fragmentation of analyte compounds, ESI-MS has been employed in several studies to probe SOA composition (Bateman et al., 2008, 2012; Walser et al., 2008; Doezema et al., 2012). The HPLC-ESI-MS system used here consists of an Agilent 1100 Series liquid chromatograph coupled to an Agilent LC/MCD TOF G1969A time-of-flight mass spectrometer with an electrospray ionization source. The chromatographic separation occurred on a Kinetex 100x3 mm C18 column with 2.6 μm particle size and a sample injection volume of 50 μL at a flow rate of 0.5 mL/min. The electrospray ionization system had a nebulizer gas pressure of 50 psi and an electrospray voltage of 3000 V. High mass resolution (m/Δm varies between 5000 at m/z 118 amu to 15000 at m/z 1822 amu) and chromatographic separation of the analytes allowed for straightforward identification of product molecular formulae (Desyaterik et al., 2013).

Between each experiment, the chamber was cleaned for at least 24 hours by flushing with zero air and O_3 from the source used during experiments until particle concentrations were at or below their typical background level (<1 μg m^{-3}) and NO_2 concentrations were below 5 ppb. Particle formation was never observed while O_3 and NO_2 were stabilizing for a new experiment, indicating that any traces of BVOC from the previous experiment had been sufficiently removed from the chamber.

3 Results & Discussion

3.1 Aerosol formation trends

Raw number and volume concentration time series are presented in Figure 3. These comparisons are not directly indicative of relative yields due to differences in initial monoterpene concentrations shown in Table 2 (see Section 3.2 for further discussion of aerosol mass yields). However, these

comparisons nicely illustrate the vast diversity of the behavior of each monoterpene with respect to systematically changing oxidant conditions, from O_3-dominated to NO_3-dominated. α-pinene exhibits a decrease in both the total number of particles produced (N_{tot}) and total aerosol volume produced (V_{tot}) with increasing NO_2, consistent with the findings of other studies (Perraud et al., 2012; Presto et al., 2005). β-pinene and Δ^3-carene both exhibit a similar decrease in N_{tot} with addition of NO_2 as α-pinene, but at early times in the reaction, the addition of NO_2 appears to enhance volume growth relative to the O_3-only experiment. Limonene exhibits enhancement in both N_{tot} and V_{tot} with addition of NO_2. While all three of the monoalkene monoterpenes produce fewer particles at higher [NO_2], α-pinene is the only terpene for which the aerosol production seems to be systematically depleted with the addition of NO_2. β-pinene and Δ^3-carene, in contrast, seem to level off at comparable N_{tot} values for the intermediate range of [NO_2]. All four monoterpenes exhibit suppression of aerosol formation at the highest [NO_2] studied, which is likely the result of RO_2+NO_2 chemistry becoming kinetically dominant at such high concentrations and producing metastable, less condensable peroxynitrate products (Barthelmie and Pryor, 1999).

3.2 SOA yields

While this study lacks direct BVOC measurements and thus is not optimized to rigorously measure aerosol yields, the framework of aerosol mass yields can still be used to compare aerosol formation trends between each experiment while accounting for differing initial hydrocarbon concentrations as well as differing aerosol mass loadings for each experiment. Unitless aerosol mass yields (Y) are defined as the aerosol mass produced per hydrocarbon mass consumed (Y=ΔM/ΔHC). Since the hydrocarbon was not measured online during experiments, ΔHC values were determined using the gas-phase kinetics model described in detail in the supplemental information. The modeled cumulative concentration of monoterpene reacted was converted to ΔHC in μg m^{-3} using the molecular weight of monoterpenes (136.23 g mol^{-1}). In the model, ΔHC is calculated based on how much of each oxidant reacts with the monoterpene. However, NO_3 can also react with subsequent RO_2 radicals, thus depleting the concentration available to react directly with BVOC. The rate constant used for RO_2 + NO_3 (2×10^{-12} cm^3 molec^{-1} s^{-1}) is reasonably well known and constant over a range of RO_2 structures ($1.8 \pm 1.5 \times 10^{-12}$ cm^3 molec^{-1} s^{-1} for C_2 - C_6 RO_2) (Vaughan et al., 2006). The rate constant for RO_2 + RO_2, the main competing RO_2 sink, is far more variable over RO_2 structures, though, so the "best estimate" employed in this study spans three orders of magnitude (described further in supplemental information). Therefore, $k_{RO2+RO2}$ is the largest source of uncertainty in ΔHC, and aerosol yield ranges are calculated spanning the minimum (10^{-15} cm^3 molec^{-1} s^{-1}) and maximum (10^{-12} cm^3 molec^{-1} s^{-1}) values used. Because O_3 is not expected to react with RO_2 (whereas NO_3 does), ΔHC from the O_3-only experiments does not vary in response to shifting $k_{RO2+RO2}$ values.

ΔM was determined by converting the wall loss-corrected aerosol total volume data to mass, assuming a SOA density of 1.4 g mL^{-1} (Hoyle et al., 2011). Uncertainty in ΔM was estimated using replicate measurements of α-pinene + O_3 (Expts 1 & 2 in Table 2) as described in detail in the supplemental information. The two ΔM time series were interpolated onto the same ΔHC trace, and time series of the average and standard deviation of ΔM were calculated. The deviation between these two experiments was slightly variable with time, so we conservatively chose the highest stable value – 15% relative error – to use as the ΔM precision estimate. Using the corresponding ΔM and ΔHC time series and respective uncertainties, a time series of mass yields was attainable, as shown in Figure 4, plotted against aerosol mass produced (ΔM), where ΔM and ΔHC are calculated relative to the beginning of the experiment. In some cases, namely the β-pinene + O_3 + NO_2 experiments, the aerosol growth rapidly exceeded the size range of the SEMS (20-800 nm). Aerosol data presented here is truncated as soon as the size distribution begins to exceed the range of the SEMS instrument resulting in these experiments "ending" at quite low mass loadings before the yield curves have flattened.

A variety of factors may contribute to the absolute numerical values of these yields differing from yields reported in the literature. For example, vapor phase wall losses were not accounted for (Zhang et al., 2014), and the chamber size, mixing, and conditioning of walls differ from other studies. Since these experiments were conducted without seed particles, rather than having a constant particle distribution for vapors to condense onto, size distributions emerged as freshly nucleated particles that proceeded through full growth curves until they exceeded the range of the SEMS and eventually were removed through the constant outflow of the chamber. This combination of growth and dilution led to an oscillatory behavior of periodic full growth curves as the condensational sink was changing, thus preventing a true steady state from ever being achieved. The yield curves shown in Figure 4 highlight a single growth curve for each experiment, but these yields may be more indicative of kinetically-limited growth than thermodynamic partitioning, causing them to differ from other studies. Additionally, and perhaps most importantly, the chemistry itself (including both first generation oxidation and peroxy radical fate) is expected to differ substantially in these mixed oxidant conditions compared to single oxidant studies in the literature. With all of those factors in mind, the precision reflected in the error ranges in Figure 4 gives us confidence that the relative yield comparisons between individual experiments in this study are robust.

Figure 4 enables yield comparisons at comparable mass loadings and also accounts for the fact that each experiment began with somewhat variable BVOC concentrations. We still see similar trends as were observed in the V_{tot} panels of Figure 3. Figure 4 illustrates that increasing [NO_2] substantially depletes aerosol formation from α-pinene, whereas β-pinene and Δ^3-carene have comparable yields over the full range of oxidant conditions, and limonene exhibits enhancement of aerosol formation at higher [NO_2]. It should be noted that yield calculations were only performed on the O_3-only and lowest two [NO_2] studied for each monoterpene due to difficulties in reliably reproducing ΔHC in

the kinetics model for the highest [NO_2] experiments. The model is constrained using the observed O_3 decay, but these high NO_2 experiments react nearly all the BVOC by way of NO_3, leaving the O_3 decay nearly unaffected. Furthermore, we expect the full duration of these experiments to be kinetically dominated by the RO_2+NO_2 reservoir (peroxynitrates), thus hindering SOA production. For these reasons, the high NO_2 experiments are not included in yield comparisons.

3.3 Individual oxidant contributions

Gas-phase kinetics modeling of the steady state conditions in the chamber yielded the time series of relative O_3 and NO_3 (and OH) contributions to BVOC oxidation. Since each experiment starts with O_3, NO_2, NO_3, and N_2O_5 at their equilibrium concentrations, initial BVOC oxidation will be dominated by NO_3, which reacts orders of magnitude faster than O_3 (Table 1). Eventually, as concentrations of precursors change over time, rates to each oxidant change and O_3 starts to contribute. We assume OH is produced from stabilized Criegee intermediates from ozonolysis according to the monoterpene-dependent yields found in Atkinson et al. (1992) and described in the supplemental information. The timing and relative contribution of O_3 depends on the relative rate constants of O_3 and NO_3 with each monoterpene, and thus the influence of each oxidant varies for all conditions tested.

This feature of staggered oxidant contributions is convenient to test the hypothesis that observed yield differences between different oxidant conditions applied to a single monoterpene can be attributed to distinct contributions from NO_3 and O_3 oxidation. For β-pinene (Figure 5), Δ^3-carene (Figure S.8), and limonene (Figure S.8), the fact that any aerosol mass is observed during the beginning of the NO_2 experiments when oxidation exclusively goes by way of NO_3 indicates that qualitative yield differences relative to the O_3 experiment can be attributed at least in part to NO_3 oxidation products. In contrast, Figure 5 shows that neither of the α-pinene experiments with NO_2 produce any aerosol mass until O_3 starts to contribute. This observation is consistent with the hypothesis that the observed suppression of aerosol formation from α-pinene with increasing concentrations of NO_2 can be attributed to its (near) 0% yield with NO_3 observed in other studies (Hallquist et al., 1999; Spittler et al., 2006; Fry et al., 2014).

For β-pinene, Δ^3-carene, and limonene, while it is clear that aerosol mass forms from NO_3 oxidation products in the NO_2 experiments, a time lag becomes apparent during which BVOC is reacting but no aerosol is formed. As soon as aerosol formation is initiated, however, the mass rapidly increases. The kinetics model used in this study assumes three options for RO_2 fate: reaction with RO_2, NO_3, or NO_2. In section 3.1, we propose that high NO_2 experiments yield low mass concentrations due to the formation of less stable peroxynitrates. This explanation likely accounts for the lag time observed in each NO_2 experiment before aerosol is able to form. Indeed, from the model we can calculate a ratio of RO_2+NO_2 products relative to the sum of RO_2+RO_2, RO_2+NO_3, and RO_2+NO_2 products present in the chamber at each time in the experiment. When this ratio time

series is overlaid onto the plots in Figure 5, a minimum in RO_2+NO_2 products appears at approximately the same time that aerosol formation is initiated. This timing, shown in Figure 5 and Figure S.8, indicates that even the low NO_2 experiments have enough NO_2 present that formation of relatively volatile peroxynitrates may kinetically dominate experiments at early times until RO_2+RO_2 and RO_2+NO_3 products start to compete.

The percentage of BVOC reacted by each of the three oxidants was modeled and is shown in Table 3. Comparisons were made at two hours into the reaction after the initial buildup of NO_3 and N_2O_5 was depleted and chemical production of NO_3 more realistically competes with O_3 oxidation of BVOCs. Even at this point in time, NO_3 dominates the initial oxidation pathway for all NO_2 concentrations and all monoterpenes, further indicating that if NO_3 oxidation contributes to SOA mass, as is certainly the case for β-pinene, Δ^3-carene, and limonene, these NO_3 oxidation products are plentiful enough throughout the full experiment to contribute significantly to observed yield differences between those experiments relative to the O_3-only experiments.

3.4 Bulk SOA composition

Filter samples from experiments that yielded sufficient aerosol mass (all expts in Table 2 except 1, 5, 9, 13) were collected and analyzed offline by HPLC-ESI-MS at Colorado State University. Because electrospray ionization is a soft ionization technique, this method has been shown to be especially useful for detecting a wide range of m/z products – including oligomer species that are likely to be significant SOA constituents (Walser et al., 2008; Surratt et al., 2006; Doezema et al., 2012). Although quantitative comparisons of products are not possible due to differences in mass loadings and a lack of calibration standards, qualitative differences in product distributions were readily apparent and consistent with observed aerosol yield trends.

Introducing NO_2 into ozonolysis of monoterpenes influences the composition of resulting SOA in two different ways: first, by forming NO_3 that can either oxidize BVOC directly or react with NO_3- or O_3-initiated RO_2, or second, by directly reacting with RO_2 or other products and reaction intermediates as NO_2. A visual comparison of the total ion chromatograms from ozonolysis of β-pinene with no NO_2 and the two lowest concentrations of NO_2 (Figure 6) shows that several new products form once NO_2 is added, and that in general increasing [NO_2] simply increases the intensity of those products rather than changing product identities substantially. For ease of interpretation, results from all of the NO_2-containing experiments were combined into a single product distribution from "NO_3-influenced oxidation." We can then compare those product distributions to those of the O_3-only experiments. A complete list of compound formulae detected (> 1.5% relative intensity, see supplemental information) in the O_3 and NO_3 dominated oxidation of each monoterpene is compiled in Table S.2.

To best highlight qualitative differences in the identity of molecules that make SOA for each set of precursors, every unique compound (distinct either in mass, retention time, or both) was accounted

for once, not normalized by peak intensity. A variety of average bulk composition parameters were calculated for each experiment, highlighted in Table 5, including average number of C, O, and N atoms per compound, molecular weight, and total number of products. Some artifacts may remain in this dataset, such as impurities not captured by the background subtraction or product fragments that do not reflect the original identity of the SOA product. The former should affect all samples uniformly in this analysis and thus will not influence qualitative comparisons, and the latter will either affect multiple samples and thus be irrelevant in comparisons or only affect single samples and thus still provide interesting qualitative differences.

A direct correlation between any of the average parameters (MW_{avg}, C_{avg}, O_{avg}, N_{avg}) in Table 5 and absolute aerosol yields is not obvious. α-pinene ozonolysis, for example, produced the highest aerosol mass of all the conditions tested, and while its average MW and number of C atoms are higher than ozonolysis from all the other monoterpenes, those same values are comparable to each of the NO_3 experiments, and substantially lower than those values for limonene + NO_3. However, the difference in average values, defined as the difference in each average parameter between O_3 and NO_3 dominated oxidation for each monoterpene (Δ_{avg}), are consistent with O_3 vs. NO_3 yield comparisons. β-pinene and Δ^3-carene have similar Δ_{avg} values for each parameter (as well as similar absolute values for each oxidant condition), suggesting that the addition of NO_3 affects the product distribution of these two monoterpenes similarly. The Δ_{avg} values for limonene are much higher than any other monoterpene in this study, consistent with it having the highest NO_3 aerosol yields. Again, perhaps most notably, the Δ_{avg} parameters hover near zero for α-pinene, suggesting that the aerosol composition does not differ much between the two oxidants – consistent with all of α-pinene aerosol production coming exclusively from O_3-oxidation.

To illustrate some of the finer detail of these product distributions, Figure 7 shows histograms where each observed product is binned by compound mass, in 50 amu intervals. Every experiment shows some contribution from oligomer products (m/z > 246, according to Perraud et al. (2010), >300 according to Walser et al. (2008)), but this contribution is most pronounced from NO_3 oxidation of β-pinene, Δ^3-carene, and limonene. In particular, we observe substantially more distinct products >400 amu from β-pinene, Δ^3-carene, and limonene with the O_3 / NO_2 / NO_3 mixture than from O_3 alone. In this region, the mass distributions for α-pinene in both oxidant conditions are identical. Since mass is an important contributing factor to volatility (e.g. Donahue et al. (2011)), these high mass products are likely important in aerosol formation and growth, and thus may be explanatory of the observed yield differences from NO_3-oxidation. If oligomerization is an important pathway leading to SOA formation and growth from NO_3-initiated chemistry, α-pinene's lack of oligomer products with NO_3 may be responsible for its 0% aerosol yield. In contrast, comparison of the four O_3-only histograms shows relatively small contributions of high MW oligomers for any monoterpene, in spite of quite high aerosol yields in some cases, indicating that aerosol formation by ozonolysis may not require oligomerization.

Recent studies of SOA nucleation and growth from ozonolysis of α-pinene have shown that highly oxidized and/or oligomeric species are likely important in nucleation and early growth, but that growth beginning around 20 nm is dominated by lower MW products (140-380 amu) (Zhao et al., 2013; Winkler et al.). This latter MW range is consistent with the ozonolysis products we observe for all four monoterpenes, indicating that high MW products may dominate only early stages of growth and are thus not detectable at the high mass loadings in this study. NO_3 oxidation, on the other hand, seems to provide a weaker source of low volatility compounds contributing to nucleation and early growth, as seen in the decrease of N_{tot} with increasing [NO_2] in Figure 3 (with the exception of limonene), but produces oligomers throughout the full time period of aerosol growth, leading to total aerosol mass concentrations that rival ozonolysis (with the exception of α-pinene), as seen in Figure 4. Further supporting this observed difference in products from ozonolysis compared to NO_3 oxidation is the difference in the reaction rate of each process. O_3 + BVOC is much slower than NO_3 + BVOC, which means that RO_2 is produced more slowly from ozonolysis and thus the RO_2 lifetime is much longer with respect to other radical species. Longer RO_2 lifetimes are more conducive to isomerization processes like autoxidation (Crounse et al., 2013; Jokinen et al., 2014), which may be responsible for the initial high MW nucleating species observed in other ozonolysis studies. In contrast, NO_3 oxidation produces RO_2 much more rapidly, therefore increasing the likelihood of RO_2 + RO_2 oligomerization.

Mass spectra alone provide limited compositional information since they do not distinguish between different functional groups. However, in this system, one functional group that can be easily parsed out of the data is the nitrate group. From the NO_3 initiated oxidation chemistry, we expect that any nitrogen present in a molecule is a part of a nitrate functional group. (Some instances of –NO and –ONO have been found in the compound list, causing relatively high N_{avg} values for α-pinene + O_3, for example, where we expect any nitrogen is due to impurities.) The Δ_{avg} values in Table 5 for N_{avg} provide an approximate estimate of relative aerosol organic nitrate yield. β-pinene, Δ^3-carene, and limonene all exhibit a substantial increase in average number of N per molecule with the addition of NO_2, consistent with the relatively high organic nitrate yields observed from NO_3 oxidation of those species in other studies (Fry et al., 2014; Hallquist et al., 1999). α-pinene produces comparatively fewer nitrogen-containing SOA products in the presence of NO_2. While the organic nitrate products from α-pinene may be relatively volatile and thus not partition appreciably into the aerosol phase, it is clear that this is not a universal characteristic of C_{10} organic nitrates, as many do partition into the aerosol phase for all three other monoterpenes studied – even those with relatively low total aerosol mass loading.

We note that the products observed here from ozonolysis vs. NO_3 oxidation are consistent with proposed mechanisms in the literature. Table S.3 includes proposed structures for several masses that have been observed in other studies, including several monomeric carboxylic acids and aldehydes from ozonolysis (Glasius et al., 2000; Yu et al., 1999) as well as multi-functional monomeric nitrates

from NO_3-oxidation (Wangberg et al., 1997; Perraud et al., 2010), some of which have been included in Figure 6 to highlight relative intensities across different NO_2 conditions. Several more speculative structures are shown in the supplemental information to indicate that observed oligomeric masses can be reasonably achieved from dimers of first generation oxidation products.

4 Implications: determination of dominant nighttime oxidant using NO_2 to BVOC ratio

Using literature rate constant data (Table 1), we can approximate the NO_2/BVOC regime where NO_3 will dominate nighttime oxidation for each monoterpene. Since O_3 contributes to both NO_3 formation and BVOC-oxidation, and for all monoterpenes NO_3 oxidation is much faster than O_3 oxidation, we assume that once NO_3 production becomes faster than O_3 oxidation of BVOC (Eq. 1), NO_3 becomes the dominant oxidant. The ratio of NO_2/BVOC at which this crossover occurs, defined in Eq. 2, is calculated for each monoterpene and reported in Table 4.

$$k_{(O_3+NO_2)}[O_3][NO_2] > k_{(O_3+BVOC)}[O_3][BVOC] \tag{1}$$

$$\frac{[NO_2]}{[BVOC]} > \frac{k_{(O_3+BVOC)}}{k_{(O_3+NO_2)}} \tag{2}$$

This calculation leaves out factors like competing sinks for NO_3 and is thus a very crude approximation. Nevertheless, it is noteworthy how small the magnitude of these ratios are. Figure 8 shows diurnally averaged NO_2 and bulk monoterpene concentrations from two field campaigns: BEACHON-RoMBAS in 2011, which took place in a remote montane forested location in the Rocky Mountain front range (Fry et al., 2013), and SOAS in 2013, which took place in a rural subtropical forest region in central Alabama (Ayres et al., 2015). Across both of these campaigns, NO_2 and total monoterpene diurnal concentrations were qualitatively and quantitatively similar. For the BEACHON-RoMBAS campaign, we assume that the average monoterpene distribution was 1:1:1 α-pinene:β-pinene:Δ^3-carene (Fry et al., 2013), whereas at SOAS we have explicit speciated monoterpene measurements. For each campaign, we calculated the average diurnal cycle of [NO_2]/[BVOC] using speciated monoterpene concentrations. The dashed lines indicate the minimum calculated threshold from Table 4, above which NO_3 oxidation is expected to dominate over O_3 oxidation. The shaded nighttime portions of Figure 8 show measured average [NO_2]/[BVOC] ratios exceeding the minimum threshold at all times during the BEACHON-RoMBAS campaign, and at all times for β-pinene and limonene at SOAS as well as part of the night for α-pinene at SOAS.

These ratios are expected to be even higher in regions with stronger anthropogenic influences. This analysis suggests that NO_3 is not only a relevant contributor to nighttime oxidation chemistry, it may actually dominate oxidation pathways in many regions. The consequence of this NO_3-dominant oxidation chemistry for SOA formation downwind of large NO_x point sources (coal-fired power

plants) has been recently investigated (Fry et al., 2015), showing spatial patterns of predicted SOA production that depend substantially on the forest surrounding the point source. The present study expands on this thinking to include further downwind regions where O_3 and NO_3 begin to compete. If NO_3 contributes significantly to oxidation pathways in ambient air over a wide range of NO_2 concentrations, the fact that each monoterpene displays vastly different aerosol yields from NO_3 vs O_3 oxidation and that this difference differs among monoterpenes becomes essential to accurately predicting aerosol formation in different regions.

5 Conclusions

This work adds to the growing body of monoterpene aerosol yield comparison literature suggesting that monoterpene oxidation has widely varying aerosol yields depending on the specific monoterpene and oxidant combination (Fry et al., 2014; Griffin et al., 1999; Hallquist et al., 1999; Ng et al., 2006; Glasius et al., 2000; Yu et al., 1999; Lee et al.). We therefore conclude, first and foremost, that there is no single "representative" monoterpene. Furthermore, the monoterpene most often considered representative of BVOC oxidation, α-pinene, presents here as the greatest anomaly with respect to aerosol formation, showing higher ozonolysis aerosol mass yields than even limonene, and behaving in a way consistent with 0 % aerosol yields from reaction with NO_3.

We show that under the influence of NO_3, α-pinene produces comparatively few condensed phase organic nitrates and oligomers with respect to the other three monoterpenes studied. This finding is consistent with α-pinene's negligible aerosol yield with NO_3 and also suggests more generally that oligomers and multifunctional organic nitrates are important products leading to SOA formation from NO_3. Additionally, the difference in product distributions between O_3 and NO_3 oxidation for all monoterpenes studied (except α-pinene) indicates that each oxidant broadly employs a different mechanism toward condensable products – O_3 likely nucleates and grows enough aerosol mass early in the reaction that subsequent condensation is governed by comparatively small molecular weight species, whereas NO_3 produces less extremely low volatility material early but produces oligomers consistently throughout the period of condensation such that they constitute an observable fraction of the bulk aerosol.

Careful treatment of the first generation kinetics of this atmospherically relevant nighttime oxidant mixture also served to contextualize the relative importance of each observed aerosol precursor in different regions. We propose using NO_2/BVOC ratios for each monoterpene to predict the dominant nighttime oxidation pathway for each (Table 4). For example, for β-pinene at NO_2/BVOC ratios greater than 0.47, NO_3 oxidation will begin to out-compete O_3 oxidation, suggesting that β-pinene oxidation by O_3 is likely to be minor at night in all but the most pristine environments. β-pinene displays a rather extreme manifestation of this observation, but all four monoterpenes studied have NO_2/BVOC ratios such that NO_3 oxidation is likely to dominate even in relatively remote regions.

The complexity shown by just these four BVOCs reacting with two different oxidants suggests that bulk parameters in global and regional models need to be very carefully considered if they are going to accurately match observed ambient organic aerosol loadings. These models use one or two, typically daytime, aerosol yield parameters for bulk monoterpenes – often considering α-pinene or β-pinene yields to be representative (e.g. Lane et al. (2008)). To the knowledge of the authors, the modeling approaches of Hoyle et al. (2007) and Pye et al. (2010) are the only global-scale models that parameterize NO_3 chemistry. Future challenges in constraining the global aerosol budget will likely require creating more nuanced approaches to modeling different regions with ostensibly similar chemistry that has been shown to have diverse effects on aerosol formation.

Acknowledgements. JLF and DCD gratefully acknowledge funding from the National Center for Environmental Research (NCER) STAR Program, EPA#RD-83539901 as well as the Reed College Class of '21 Award. We thank Rhiana Meade for development of the RECv1.0 as well as Dean Atkinson for donation of PFA film to build the RECv2.0 used in this study. DKF acknowledges the National Science Foundation (AGS 1240611) for support.

References

Atkinson, R. and Arey, J.: Atmospheric Degradation of Volatile Organic Compounds, Chemical Reviews, 103, 4605–4638, doi:10.1021/cr0206420, http://pubs.acs.org/doi/abs/10.1021/cr0206420, 2003.

Atkinson, R., Aschmann, S. M., Arey, J., and Shorees, B.: Formation of OH radicals in the gas phase reactions of O_3 with a series of terpenes, Journal of Geophysical Research: Atmospheres, 97, 6065–6073, doi:10.1029/92JD00062, http://dx.doi.org/10.1029/92JD00062, 1992.

Ayres, B. R., Allen, H. M., Draper, D. C., Brown, S. S., Wild, R. J., Jimenez, J. L., Day, D. A., Campuzano-Jost, P., Hu, W., de Gouw, J., Koss, A., Cohen, R. C., Duffey, K. C., Romer, P., Baumann, K., Edgerton, E., Takahama, S., Thornton, J. A., Lee, B. H., Lopez-Hilfiker, F. D., Mohr, C., Goldstein, A. H., Olson, K., and Fry, J. L.: Organic nitrate aerosol formation via NO_3 + BVOC in the Southeastern US, Atmospheric Chemistry and Physics Discussions, 15, 16 235–16 272, doi:10.5194/acpd-15-16235-2015, http://www.atmos-chem-phys-discuss.net/15/16235/2015/, 2015.

Barthelmie, R. J. and Pryor, S. C.: A model mechanism to describe oxidation of monoterpenes leading to secondary organic aerosol: 1. α-pinene and β-pinene, Journal of Geophysical Research: Atmospheres, 104, 23 657–23 699, doi:10.1029/1999JD900382, http://dx.doi.org/10.1029/1999JD900382, 1999.

Bateman, A. P., Walser, M. L., Desyaterik, Y., Laskin, J., Laskin, A., and Nizkorodov, S. A.: The Effect of Solvent on the Analysis of Secondary Organic Aerosol Using Electrospray Ionization Mass Spectrometry, Environmental Science & Technology, 42, 7341–7346, doi:10.1021/es801226w, http://pubs.acs.org/doi/abs/10.1021/es801226w, 2008.

Bateman, A. P., Laskin, J., Laskin, A., and Nizkorodov, S. A.: Applications of High-Resolution Electrospray Ionization Mass Spectrometry to Measurements of Average Oxygen to Carbon Ratios in Secondary Organic Aerosols, Environmental Science & Technology, 46, 8315–8324, doi:10.1021/es3017254, http://pubs.acs.org/doi/abs/10.1021/es3017254, 2012.

Boyd, C. M., Sanchez, J., Xu, L., Eugene, A. J., Nah, T., Tuet, W. Y., Guzman, M. I., and Ng, N. L.: Secondary organic aerosol formation from the β-pinene+NO_3 system: effect of humidity and peroxy radical fate, Atmospheric Chemistry and Physics, 15, 7497–7522, doi:10.5194/acp-15-7497-2015, http://www.atmos-chem-phys.net/15/7497/2015/, 2015.

Carlton, A. G., Pinder, R. W., Bhave, P. V., and Pouliot, G. A.: To What Extent Can Biogenic SOA be Controlled?, Environmental Science & Technology, 44, 3376–3380, doi:10.1021/es903506b, http://pubs.acs.org/doi/abs/10.1021/es903506b, 2010.

Crounse, J. D., Nielsen, L. B., Jørgensen, S., Kjaergaard, H. G., and Wennberg, P. O.: Autoxidation of Organic Compounds in the Atmosphere, The Journal of Physical Chemistry Letters, 4, 3513–3520, doi:10.1021/jz4019207, http://dx.doi.org/10.1021/jz4019207, 2013.

Davidson, C. I., Phalen, R. F., and Solomon, P. A.: Airborne Particulate Matter and Human Health: A Review, Aerosol Science and Technology, 39, 737–749, doi:10.1080/02786820500191348, http://www.tandfonline.com/doi/abs/10.1080/02786820500191348, 2005.

Desyaterik, Y., Sun, Y., Shen, X., Lee, T., Wang, X., Wang, T., and Collett, J. L.: Speciation of "brown" carbon in cloud water impacted by agricultural biomass burning in eastern China, Journal of Geophysical Research: Atmospheres, 118, 7389–7399, doi:10.1002/jgrd.50561, http://dx.doi.org/10.1002/jgrd.50561, 2013.

Doezema, L. A., Longin, T., Cody, W., Perraud, V., Dawson, M. L., Ezell, M. J., Greaves, J., Johnson, K. R., and Finlayson-Pitts, B. J.: Analysis of secondary organic aerosols in air using extractive electrospray ionization mass spectrometry (EESI-MS), RSC Adv., 2, 2930–2938, doi:10.1039/C2RA00961G, http://dx.doi.org/10.1039/C2RA00961G, 2012.

Donahue, N. M., Epstein, S. A., Pandis, S. N., and Robinson, A. L.: A two-dimensional volatility basis set: 1. organic-aerosol mixing thermodynamics, Atmospheric Chemistry and Physics, 11, 3303–3318, doi:10.5194/acp-11-3303-2011, http://www.atmos-chem-phys.net/11/3303/2011/, 2011.

Ehn, M., Thornton, J. A., Kleist, E., Sipila, M., Junninen, H., Pullinen, I., Springer, M., Rubach, F., Tillmann, R., Lee, B., Lopez-Hilfiker, F., Andres, S., Acir, I.-H., Rissanen, M., Jokinen, T., Schobesberger, S., Kangasluoma, J., Kontkanen, J., Nieminen, T., Kurten, T., Nielsen, L. B., Jorgensen, S., Kjaergaard, H. G., Canagaratna, M., Maso, M. D., Berndt, T., Petaja, T., Wahner, A., Kerminen, V.-M., Kulmala, M., Worsnop, D. R., Wildt, J., and Mentel, T. F.: A large source of low-volatility secondary organic aerosol, Nature, 506, 476–479, doi:10.1038/nature13032, http://dx.doi.org/10.1038/nature13032, 2014.

Fry, J. L., Kiendler-Scharr, A., Rollins, A. W., Wooldridge, P. J., Brown, S. S., Fuchs, H., Dubé, W., Mensah, A., dal Maso, M., Tillmann, R., Dorn, H.-P., Brauers, T., and Cohen, R. C.: Organic nitrate and secondary organic aerosol yield from NO_3 oxidation of β-pinene evaluated using a gas-phase kinetics/aerosol partitioning model, Atmospheric Chemistry and Physics, 9, 1431–1449, doi:10.5194/acp-9-1431-2009, http://www.atmos-chem-phys.net/9/1431/2009/, 2009.

Fry, J. L., Kiendler-Scharr, A., Rollins, A. W., Brauers, T., Brown, S. S., Dorn, H.-P., Dubé, W. P., Fuchs, H., Mensah, A., Rohrer, F., Tillmann, R., Wahner, A., Wooldridge, P. J., and Cohen, R. C.: SOA from limonene: role of NO_3 in its generation and degradation, Atmospheric Chemistry and Physics, 11, 3879–3894, doi:10.5194/acp-11-3879-2011, http://www.atmos-chem-phys.net/11/3879/2011/, 2011.

Fry, J. L., Draper, D. C., Zarzana, K. J., Campuzano-Jost, P., Day, D. A., Jimenez, J. L., Brown, S. S., Cohen, R. C., Kaser, L., Hansel, A., Cappellin, L., Karl, T., Hodzic Roux, A., Turnipseed, A., Cantrell, C., Lefer, B. L., and Grossberg, N.: Observations of gas- and aerosol-phase organic nitrates at BEACHON-RoMBAS 2011, Atmospheric Chemistry and Physics, 13, 8585–8605, doi:10.5194/acp-13-8585-2013, http://www.atmos-chem-phys.net/13/8585/2013/, 2013.

Fry, J. L., Draper, D. C., Barsanti, K. C., Smith, J. N., Ortega, J., Winkler, P. M., Lawler, M. J., Brown, S. S., Edwards, P. M., Cohen, R. C., and Lee, L.: Secondary Organic Aerosol Formation and Organic Nitrate Yield from NO_3 Oxidation of Biogenic Hydrocarbons, Environmental Science & Technology, 48, 11 944–11 953, doi:10.1021/es502204x, http://dx.doi.org/10.1021/es502204x, pMID: 25229208, 2014.

Fry, J. L., Koski, C., Bott, K., Hsu-Flanders, R., and Hazell, M.: Downwind particulate matters: Regulatory implications of secondary aerosol formation from the interaction of nitrogen oxides and tree emissions, Environmental Science Policy, 50, 180 – 190, doi:http://dx.doi.org/10.1016/j.envsci.2015.02.017, http://www.sciencedirect.com/science/article/pii/S1462901115000489, 2015.

Geron, C., Rasmussen, R., Arnts, R. R., and Guenther, A.: A review and synthesis of monoterpene speciation from forests in the United States, Atmospheric Environment, 34, 1761 – 1781, doi:10.1016/S1352-2310(99)00364-7, http://www.sciencedirect.com/science/article/pii/S1352231099003647, 2000.

Glasius, M., Lahaniati, M., Calogirou, A., Di Bella, D., Jensen, N. R., Hjorth, J., Kotzias, D., and Larsen, B. R.: Carboxylic Acids in Secondary Aerosols from Oxidation of Cyclic Monoterpenes by Ozone, Environ-

mental Science & Technology, 34, 1001–1010, doi:10.1021/es990445r, http://pubs.acs.org/doi/abs/10.1021/es990445r, 2000.

Goldstein, A. H. and Galbally, I. E.: Known and Unexplored Organic Constituents in the Earth's Atmosphere, Environmental Science & Technology, 41, 1514–1521, doi:10.1021/es072476p, http://pubs.acs.org/doi/abs/10.1021/es072476p, 2007.

Griffin, R. J., Cocker, D. R., Flagan, R. C., and Seinfeld, J. H.: Organic aerosol formation from the oxidation of biogenic hydrocarbons, Journal of Geophysical Research: Atmospheres, 104, 3555–3567, doi:10.1029/1998JD100049, http://dx.doi.org/10.1029/1998JD100049, 1999.

Grosjean, D. and Harrison, J.: Response of chemiluminescence NOx analyzers and ultraviolet ozone analyzers to organic air pollutants, Environmental Science & Technology, 19, 862–865, doi:10.1021/es00139a016, http://dx.doi.org/10.1021/es00139a016, pMID: 22196613, 1985.

Guenther, A., Hewitt, C. N., Erickson, D., Fall, R., Geron, C., Graedel, T., Harley, P., Klinger, L., Lerdau, M., Mckay, W. A., Pierce, T., Scholes, B., Steinbrecher, R., Tallamraju, R., Taylor, J., and Zimmerman, P.: A global model of natural volatile organic compound emissions, Journal of Geophysical Research: Atmospheres, 100, 8873–8892, doi:10.1029/94JD02950, http://dx.doi.org/10.1029/94JD02950, 1995.

Hallquist, M., Wängberg, I., Ljungström, E., Barnes, I., and Becker, K.-H.: Aerosol and Product Yields from NO_3 Radical-Initiated Oxidation of Selected Monoterpenes, Environmental Science Technology, 33, 553–559, doi:10.1021/es980292s, http://pubs.acs.org/doi/abs/10.1021/es980292s, 1999.

Hallquist, M., Wenger, J. C., Baltensperger, U., Rudich, Y., Simpson, D., Claeys, M., Dommen, J., Donahue, N. M., George, C., Goldstein, A. H., Hamilton, J. F., Herrmann, H., Hoffmann, T., Iinuma, Y., Jang, M., Jenkin, M. E., Jimenez, J. L., Kiendler-Scharr, A., Maenhaut, W., McFiggans, G., Mentel, T. F., Monod, A., Prévôt, A. S. H., Seinfeld, J. H., Surratt, J. D., Szmigielski, R., and Wildt, J.: The formation, properties and impact of secondary organic aerosol: current and emerging issues, Atmospheric Chemistry and Physics, 9, 5155–5236, doi:10.5194/acp-9-5155-2009, http://www.atmos-chem-phys.net/9/5155/2009/, 2009.

Haynes, W., Bruno, T. J., and Lide, D. R., eds.: CRC Handbook of Chemistry and Physics, 93rd Edition (Internet Version), CRC Press/Taylor and Francis, 2012.

Heald, C. L., Jacob, D. J., Park, R. J., Russell, L. M., Huebert, B. J., Seinfeld, J. H., Liao, H., and Weber, R. J.: A large organic aerosol source in the free troposphere missing from current models, Geophysical Research Letters, 32, 4, doi:10.1029/2005GL023831, http://www.agu.org/pubs/crossref/2005/2005GL023831.shtml, 2005.

Heald, C. L., Coe, H., Jimenez, J. L., Weber, R. J., Bahreini, R., Middlebrook, A. M., Russell, L. M., Jolleys, M., Fu, T.-M., Allan, J. D., Bower, K. N., Capes, G., Crosier, J., Morgan, W. T., Robinson, N. H., Williams, P. I., Cubison, M. J., DeCarlo, P. F., and Dunlea, E. J.: Exploring the vertical profile of atmospheric organic aerosol: comparing 17 aircraft field campaigns with a global model, Atmospheric Chemistry and Physics, 11, 12 673–12 696, doi:10.5194/acp-11-12673-2011, http://www.atmos-chem-phys.net/11/12673/2011/, 2011.

Hoffmann, T., Odum, J., Bowman, F., Collins, D., Klockow, D., Flagan, R., and Seinfeld, J.: Formation of organic aerosols from the oxidation of biogenic hydrocarbons, Journal of Atmospheric Chemistry, 26, 189–222, 1997.

Hoyle, C. R., Berntsen, T., Myhre, G., and Isaksen, I. S. A.: Secondary organic aerosol in the global aerosol - chemical transport model Oslo CTM2, Atmospheric Chemistry and Physics, 7, 5675–5694, doi:10.5194/acp-7-5675-2007, http://www.atmos-chem-phys.net/7/5675/2007/, 2007.

Hoyle, C. R., Boy, M., Donahue, N. M., Fry, J. L., Glasius, M., Guenther, A., Hallar, A. G., Huff Hartz, K., Petters, M. D., Petäjä, T., Rosenoern, T., and Sullivan, A. P.: A review of the anthropogenic influence on biogenic secondary organic aerosol, Atmospheric Chemistry and Physics, 11, 321–343, doi:10.5194/acp-11-321-2011, http://www.atmos-chem-phys.net/11/321/2011/, 2011.

IPCC: Climate Change 2013: The Physical Science Basis. Contribution of Working Group I to the Fifth Assessment Report of the Intergovernmental Panel on Climate Change, Cambridge University Press, Cambridge, United Kingdom and New York, NY, USA, doi:10.1017/CBO9781107415324, www.climatechange2013.org, 2013.

Jokinen, T., Sipilä, M., Richters, S., Kerminen, V.-M., Paasonen, P., Stratmann, F., Worsnop, D., Kulmala, M., Ehn, M., Herrmann, H., and Berndt, T.: Rapid Autoxidation Forms Highly Oxidized RO2 Radicals in the Atmosphere, Angewandte Chemie International Edition, 53, 14 596–14 600, doi:10.1002/anie.201408566, http://dx.doi.org/10.1002/anie.201408566, 2014.

Kroll, J. H. and Seinfeld, J. H.: Chemistry of secondary organic aerosol: Formation and evolution of low-volatility organics in the atmosphere, Atmospheric Environment, 42, 3593 – 3624, doi:10.1016/j.atmosenv.2008.01.003, http://www.sciencedirect.com/science/article/pii/S1352231008000253, 2008.

Lane, T. E., Donahue, N. M., and Pandis, S. N.: Effect of NOx on Secondary Organic Aerosol Concentrations, Environmental Science & Technology, 42, 6022–6027, doi:10.1021/es703225a, http://dx.doi.org/10.1021/es703225a, pMID: 18767660, 2008.

Lee, A., Goldstein, A. H., Kroll, J. H., Ng, N. L., Varutbangkul, V., Flagan, R. C., and Seinfeld, J. H.: Gas-phase products and secondary aerosol yields from the photooxidation of 16 different terpenes, Journal of Geophysical Research: Atmospheres, 111, doi:10.1029/2006JD007050, http://dx.doi.org/10.1029/2006JD007050.

McMurry, P. H. and Grosjean, D.: Gas and aerosol wall losses in Teflon film smog chambers, Environmental Science amp; Technology, 19, 1176–1182, doi:10.1021/es00142a006, 1985.

Middleton, P.: Sources of air pollutants, in: Composition, Chemistry, and Climate of the Atmosphere, edited by Singh, H. B., Van Nostrand Reinhold, New York, 1995.

Moldanova, J. and Ljungström, E.: Modelling of particle formation from NO_3 oxidation of selected monoterpenes, Journal of Aerosol Science, 21, 1317–1333, doi:10.1016/S0021-8502(00)00041-0, http://www.sciencedirect.com/science/article/pii/S0021850200000410, 2000.

Ng, N. L., Kroll, J. H., Keywood, M. D., Bahreini, R., Varutbangkul, V., Flagan, R. C., Seinfeld, J. H., Lee, A., and Goldstein, A. H.: Contribution of First- versus Second-Generation Products to Secondary Organic Aerosols Formed in the Oxidation of Biogenic Hydrocarbons, Environmental Science Technology, 40, 2283–2297, doi:10.1021/es052269u, http://pubs.acs.org/doi/abs/10.1021/es052269u, 2006.

Perraud, V., Bruns, E. A., Ezell, M. J., Johnson, S. N., Greaves, J., and Finlayson-Pitts, B. J.: Identification of Organic Nitrates in the NO_3 Radical Initiated Oxidation of α-Pinene by Atmospheric Pressure Chemical Ionization Mass Spectrometry, Environmental Science Technology, 44, 5887–5893, doi:10.1021/es1005658, http://pubs.acs.org/doi/abs/10.1021/es1005658, 2010.

Perraud, V., Bruns, E. A., Ezell, M. J., Johnson, S. N., Yu, Y., Alexander, M. L., Zelenyuk, A., Imre, D., Chang, W. L., Dabdub, D., Pankow, J. F., and Finlayson-Pitts, B. J.: Nonequilibrium atmospheric secondary organic aerosol formation and growth, Proceedings of the National Academy of Sciences, 109, 2836–2841, doi:10.1073/pnas.1119909109, http://www.pnas.org/content/109/8/2836.abstract, 2012.

Pope III, C. A., Bates, D. V., and Raizenne, M. E.: Health Effects of Particulate Air Pollution: Time for Reassessment?, Environmental Health Perspectives, 103, 472–480, doi:10.2307/3432586, http://www.jstor.org/stable/3432586, 1995.

Presto, A. A., Huff Hartz, K. E., and Donahue, N. M.: Secondary Organic Aerosol Production from Terpene Ozonolysis. 2. Effect of NOx Concentration, Environmental Science Technology, 39, 7046–7054, 2005.

Pye, H. O. T., Chan, A. W. H., Barkley, M. P., and Seinfeld, J. H.: Global modeling of organic aerosol: the importance of reactive nitrogen (NO_x and NO_3), Atmospheric Chemistry and Physics, 10, 11 261–11 276, doi:10.5194/acp-10-11261-2010, http://www.atmos-chem-phys.net/10/11261/2010/, 2010.

Reis, S., Pinder, R. W., Zhang, M., Lijie, G., and Sutton, M. A.: Reactive nitrogen in atmospheric emission inventories, Atmospheric Chemistry and Physics, 9, 7657–7677, doi:10.5194/acp-9-7657-2009, http://www.atmos-chem-phys.net/9/7657/2009/, 2009.

Rollins, A. W., Browne, E. C., Min, K.-E., Pusede, S. E., Wooldridge, P. J., Gentner, D. R., Goldstein, A. H., Liu, S., Day, D. A., Russell, L. M., and Cohen, R. C.: Evidence for NOx Control over Nighttime SOA Formation, Science, 337, 1210–1212, doi:10.1126/science.1221520, http://www.sciencemag.org/content/337/6099/1210.abstract, 2012.

Sakulyanontvittaya, T., Duhl, T., Wiedinmyer, C., Helmig, D., Matsunaga, S., Potosnak, M., Milford, J., and Guenther, A.: Monoterpene and Sesquiterpene Emission Estimates for the United States, Environmental Science & Technology, 42, 1623–1629, doi:10.1021/es702274e, http://dx.doi.org/10.1021/es702274e, pMID: 18441812, 2008.

Sander, S., Abbatt, J., Barker, J. R., Burkholder, J. B., Friedl, R. R., Golden, D. M., Huie, R. E., Kolb, C. E., Kurylo, M. J., Moortgat, G. K., Orkin, V. L., and Wine, P. H.: Chemical Kinetics and Photochemical Data for Use in Atmospheric Studies, Evaluation Number 17, JPL Publication, 10, 2011.

Spittler, M., Barnes, I., Bejan, I., Brockmann, K., Benter, T., and Wirtz, K.: Reactions of NO_3 radicals with limonene and α-pinene: Product and SOA formation, Atmospheric Environment, 40, Supplement 1, 116 – 127, doi:10.1016/j.atmosenv.2005.09.093, http://www.sciencedirect.com/science/article/pii/S1352231006003268, 2006.

Surratt, J. D., Murphy, S. M., Kroll, J. H., Ng, N. L., Hildebrandt, L., Sorooshian, A., Szmigielski, R., Vermeylen, R., Maenhaut, W., Claeys, M., Flagan, R. C., and Seinfeld, J. H.: Chemical Composition of Secondary Organic Aerosol Formed from the Photooxidation of Isoprene, The Journal of Physical Chemistry A, 110, 9665–9690, doi:10.1021/jp061734m, http://dx.doi.org/10.1021/jp061734m, pMID: 16884200, 2006.

VanReken, T., Greenberg, J., Harley, P., Guenther, A., and Smith, J.: Direct measurement of particle formation and growth from the oxidation of biogenic emissions, Atmospheric Chemistry and Physics, 6, 4403–4413, doi:10.5194/acp-6-4403-2006, http://www.atmos-chem-phys.net/6/4403/2006/, 2006.

Vaughan, S., Canosa-Mas, C. E., Pfrang, C., Shallcross, D. E., Watson, L., and Wayne, R. P.: Kinetic studies of reactions of the nitrate radical (NO_3) with peroxy radicals (RO_2): an indirect source of OH at night?, Phys. Chem. Chem. Phys., 8, 3749–3760, doi:10.1039/B605569A, http://dx.doi.org/10.1039/B605569A, 2006.

Walser, M. L., Desyaterik, Y., Laskin, J., Laskin, A., and Nizkorodov, S. A.: High-resolution mass spectrometric analysis of secondary organic aerosol produced by ozonation of limonene, Phys. Chem. Chem. Phys., 10, 1009–1022, doi:10.1039/B712620D, http://dx.doi.org/10.1039/B712620D, 2008.

Wangberg, I., Barnes, I., and Becker, K. H.: Product and Mechanistic Study of the Reaction of NO_3 Radicals with α-Pinene, Environmental Science Technology, 31, 2130–2135, doi:10.1021/es960958n, http://pubs.acs.org/doi/abs/10.1021/es960958n, 1997.

Winer, A. M., Peters, J. W., Smith, J. P., and Pitts, J. N.: Response of commercial chemiluminescent nitric oxide-nitrogen dioxide analyzers to other nitrogen-containing compounds, Environmental Science Technology, 8, 1118–1121, doi:10.1021/es60098a004, http://pubs.acs.org/doi/abs/10.1021/es60098a004, 1974.

Winkler, P. M., Ortega, J., Karl, T., Cappellin, L., Friedli, H. R., Barsanti, K., McMurry, P. H., and Smith, J. N.: Identification of the biogenic compounds responsible for size-dependent nanoparticle growth, Geophysical Research Letters, 39, doi:10.1029/2012GL053253, http://dx.doi.org/10.1029/2012GL053253.

Xu, L., Guo, H., Boyd, C. M., Klein, M., Bougiatioti, A., Cerully, K. M., Hite, J. R., Isaacman-VanWertz, G., Kreisberg, N. M., Knote, C., Olson, K., Koss, A., Goldstein, A. H., Hering, S. V., de Gouw, J., Baumann, K., Lee, S.-H., Nenes, A., Weber, R. J., and Ng, N. L.: Effects of anthropogenic emissions on aerosol formation from isoprene and monoterpenes in the southeastern United States, 112, 37–42, doi:10.1073/pnas.1417609112, 2015.

Yu, J., Cocker, D., Griffin, R., Flagan, R., and Seinfeld, J.: Gas-phase ozone oxidation of monoterpenes: Gaseous and particulate products, Journal of Atmospheric Chemistry, 34, 207–258, 1999.

Zhang, X., Cappa, C. D., Jathar, S. H., McVay, R. C., Ensberg, J. J., Kleeman, M. J., and Seinfeld, J. H.: Influence of vapor wall loss in laboratory chambers on yields of secondary organic aerosol, Proceedings of the National Academy of Sciences, 111, 5802–5807, 2014.

Zhao, J., Ortega, J., Chen, M., McMurry, P. H., and Smith, J. N.: Dependence of particle nucleation and growth on high-molecular-weight gas-phase products during ozonolysis of α-pinene, Atmospheric Chemistry and Physics, 13, 7631–7644, doi:10.5194/acp-13-7631-2013, http://www.atmos-chem-phys.net/13/7631/2013/, 2013.

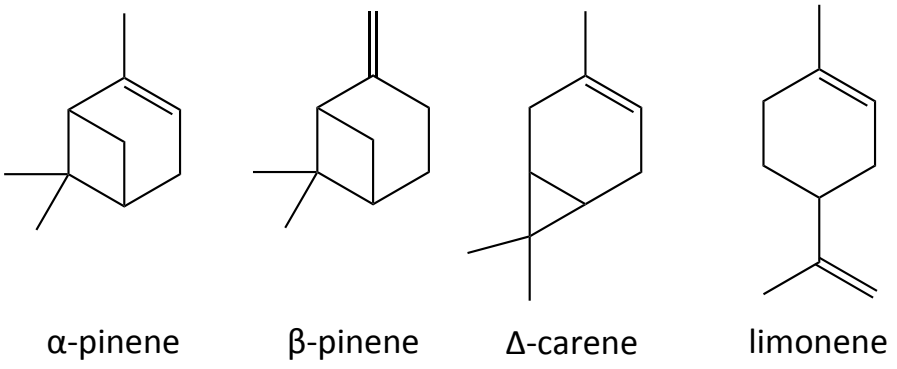

Figure 1. Structures of monoterpenes used in this study.

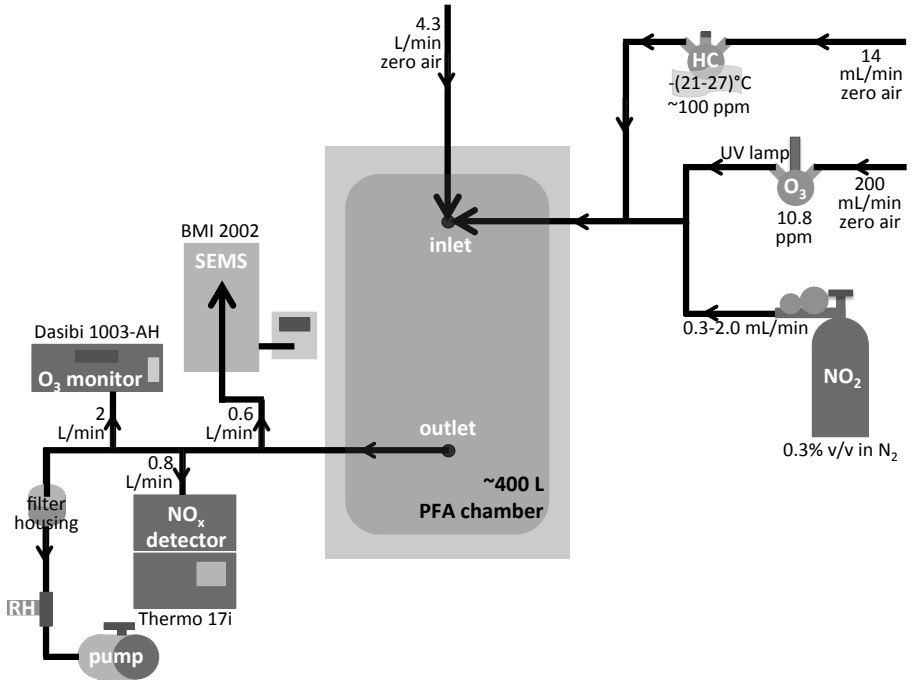

Figure 2. Reed Environmental Chamber (REC) schematic for the experiments described here.

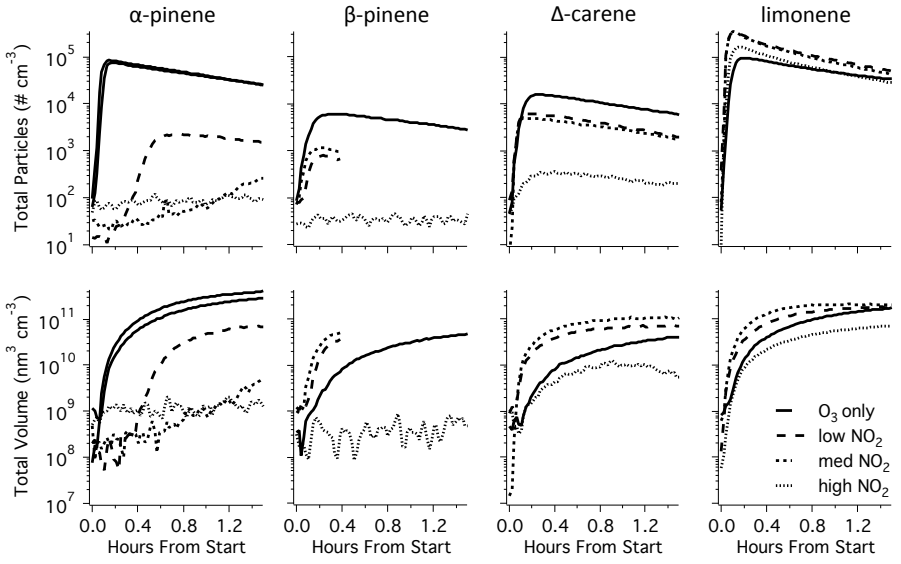

Figure 3. Raw total number concentrations (N_{tot}) and total volume concentrations (V_{tot}) at each NO_2 concentration for each monoterpene studied, not corrected for wall losses.

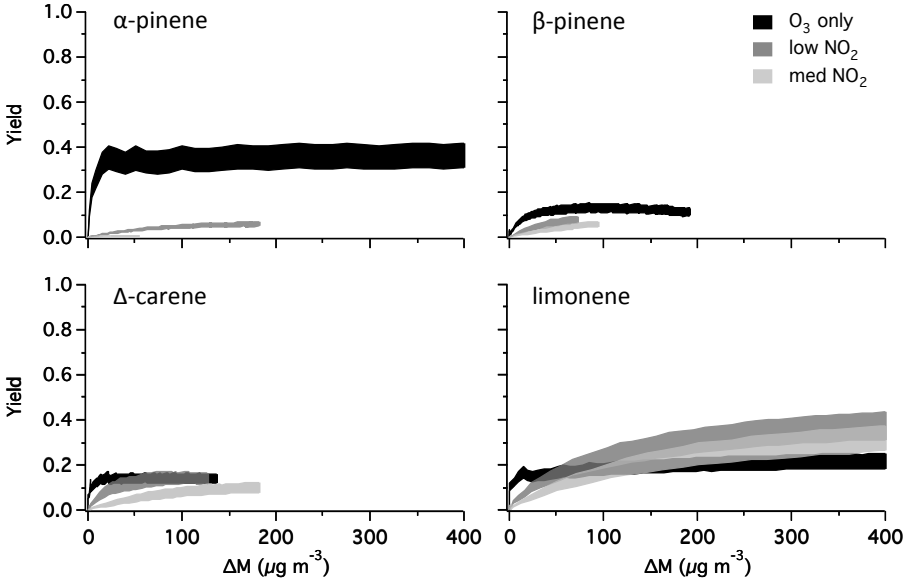

Figure 4. Yield vs ΔM for each experiment. ΔM is corrected for wall losses (described in supplemental information). Uncertainty ranges on yields arise from a constant 15% relative error on ΔM calculated based on two replicate experiments, propagated with modeled ΔHC values using the range of 10^{-15} cm^3 molec^{-1} s^{-1} to 10^{-12} cm^3 molec^{-1} s^{-1} for $k_{RO2+RO2}$ for the low and medium NO_2 experiments for each monoterpene. O_3-only experiments do not have an analogous ΔHC uncertainty range since all O_3 was assumed to react with the monoterpene directly, so uncertainty range on these traces is based exclusively on ΔM.

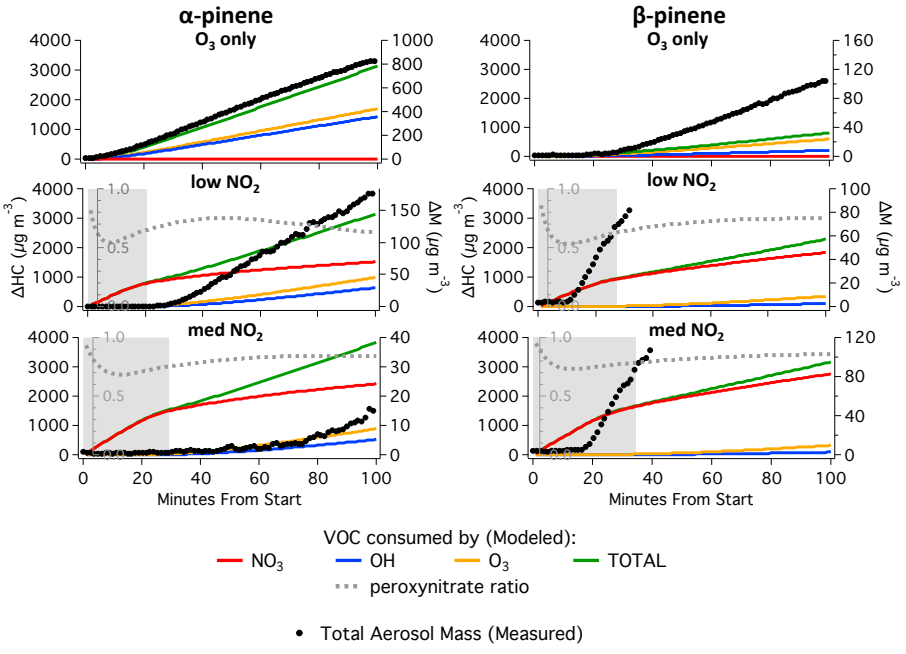

Figure 5. Time series of wall loss corrected aerosol mass (right axis) and VOC consumed by each oxidant (left axis) for α-pinene and β-pinene at zero ("O_3-only"), low, and medium NO_2 concentrations, highlighting how much aerosol is produced at times dominated by NO_3-oxidation (shaded regions). ΔHC values shown are the lower limits calculated using the lowest RO_2+RO_2 rate constant (10^{-15} cm^3 molec^{-1} s^{-1}), which gives the low limit on how much NO_3 reacts with VOC directly. Dashed grey traces (inner left grey axis) represent the ratio of RO_2+NO_2 products that are present in the chamber (instantaneous concentration) relative to the sum of the instantaneous concentrations of RO_2+RO_2, RO_2+NO_3, and RO_2+NO_2 products. This ratio is a representation of the time dependence of peroxynitrate formation in the chamber.

Table 1. Rate constants at 298 K for NO_2 + O_3 (Sander et al., 2011) and for both O_3 and NO_3 with selected monoterpenes (Atkinson and Arey, 2003).

	$k \times 10^{17}$ (cm^3 molec^{-1} s^{-1})	$k_{O3} \times 10^{17}$ (cm^3 molec^{-1} s^{-1})	$k_{NO3} \times 10^{12}$ (cm^3 molec^{-1} s^{-1})
NO_2 + O_3	3.2	–	–
α-pinene	–	8.4	6.2
β-pinene	–	1.5	2.51
Δ^3-carene	–	3.7	9.1
limonene	–	21	12.2

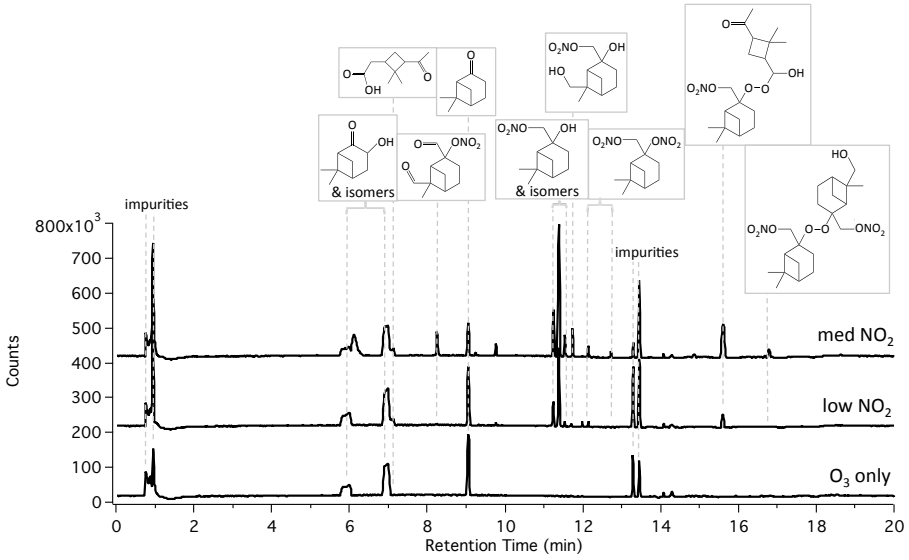

Figure 6. Comparison of chromatograms from HPLC-ESI-MS samples of SOA derived from β-pinene ozonolysis with 0 (bottom), 530 (middle), and 910 ppb NO_2 (top). Chromatograms are annotated with speculative structures corresponding to the assigned molecular formulae of the most intense peaks. Proposed structures are listed in Table S.3 based on products observed in other studies.

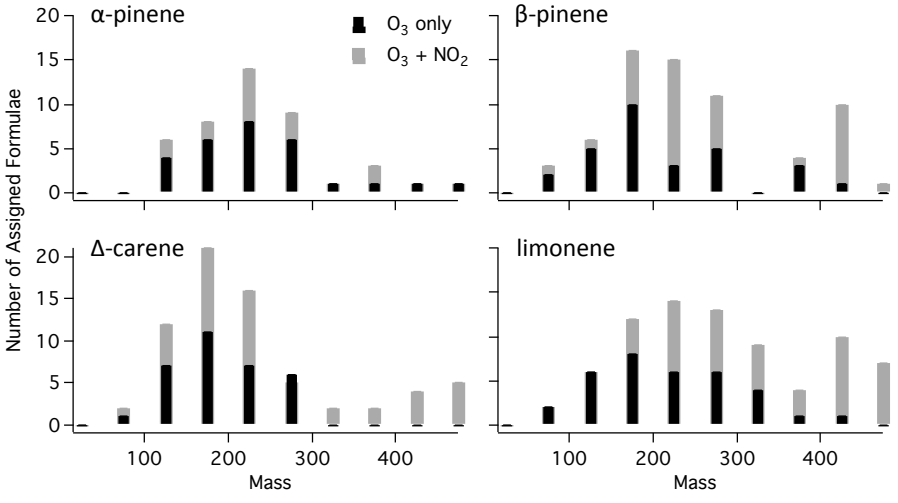

Figure 7. Histograms of each O_3 vs NO_3 (O_3 + NO_2) regime for each monoterpene showing the number of compounds (left axis) in each 50 amu mass bin (bottom axis).

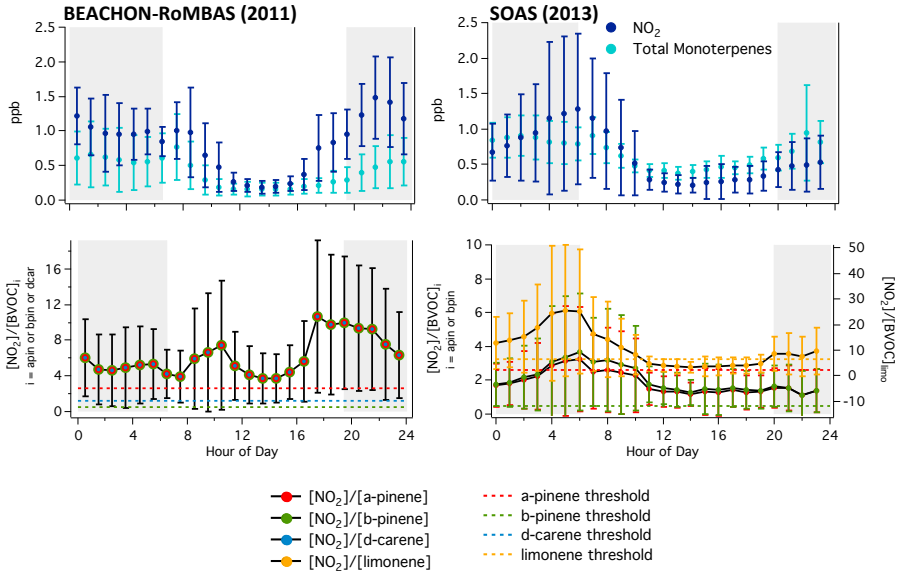

Figure 8. Diurnal average NO_2 and monoterpene concentrations (top panels) are shown for two field campaigns: BEACHON-RoMBAS 2011 (left panels) and SOAS 2013 (right panels) which both occurred at heavily biogenically influenced sites. The bottom panels show the diurnally averaged $[NO_2]$/[BVOC] ratios for the speciated monoterpenes used in this study. The speciated monoterpenes for BEACHON-RoMBAS are estimated as being 1:1:1 α-pinene:β-pinene:Δ^3-carene; hence, each BVOC concentration is assumed to be a third of total measured [BVOC]. Shaded regions indicate nighttime hours.

Table 2. Conditions for each chamber experiment.

Expt #	Date	$[BVOC]_i$* (ppb)	$[O_3]_i$ (ppb)	$[NO_2]_i$* (ppb)	RH (%)	Temp (K)	Notes
			α-pinene				
1	12/19/12	780	485	–	33	294	a
2	1/5/13	680	490	–	20	295	f
3	1/16/13	590-715	480	510	24	294	a, c
4	1/18/13	780-960	480	840	22	295	a, d
5	1/14/13	~300	480	1400	22	294	b, e
			β-pinene				
6	1/7/13	370	485	–	40	295	a
7	1/23/13	470-680	480	530	23	295	a, c
8	1/25/13	650-1100	480	910	40	295	a, b, d
9	1/21/13	~300	480	2000	20	295	b, e
			Δ-carene				
10	1/9/13	220	470	–	30	294	a
11	3/9/13	250-340	470	290	27	295	a, c
12	3/13/13	400-650	470	590	38	295	a, d
13	2/6/13	~300	470	900	33	295	b, e
			limonene				
14	1/11/13	470	485	–	20	295	a
15	3/23/13	340-400	470	360	20	295	a, c
16	3/27/13	470-560	470	720	31	295	a, d
17	3/21/13	~300	465	1000	26	295	a, b, e

*Values calculated using kinetics model.

[a] SOA filter sample collected and analyzed by HPLC-ESI-MS.

[b] [BVOC] estimated according to flow rate and temperature dependent vapor pressure within source flask.

[c] Designated "low NO_2."

[d] Designated "medium NO_2."

[e] Designated "high NO_2."

[f] Experiment included to show reproducibility of chamber.

Table 3. Percentage of total BVOC reacted by each oxidant at 2 hrs into each experiment. In the model, OH is produced from Stabilized Criegee Intermediates from ozonolysis at the following ratios: α-pinene = 0.85; β-pinene = 0.35; Δ^3-carene = 1.06; limonene = 0.86 (Atkinson et al., 1992). Values from NO_2-containing experiments include two values expressed as ***low (high)*** where "low" denotes the lower $RO_2 + RO_2$ rate constant limit (10^{-15} cm^3 molec^{-1} s^{-1}), and "high" denotes the upper limit (10^{-12} cm^3 molec^{-1} s^{-1}) as described in the supplemental information.

	$[NO_2]_i$ (ppb)	% by NO_3	% by O_3	% by OH
α-pinene	0	0	54	46
	510	44 (68)	34 (21)	22 (11)
	840	58 (78)	26 (15)	16 (7)
β-pinene	0	0	74	26
	530	77 (94)	18 (5)	5 (1)
	910	81 (95)	15 (4)	4 (1)
Δ^3-carene	0	0	49	51
	290	62 (92)	21 (5)	17 (3)
	590	63 (95)	20 (4)	17 (1)
limonene	0	0	54	46
	360	45 (74)	34 (18)	21 (8)
	720	59 (85)	26 (11)	15 (4)

Table 4. Minimum $[NO_2]$/[BVOC] value reported for each monoterpene studied at which NO_3 is expected to dominate nighttime oxidation.

BVOC	$[NO_2]$/[BVOC]
α-pinene	2.6
β-pinene	0.47
Δ^3-carene	1.2
limonene	6.6

Table 5. Average ($\pm$ one standard deviation) molecular weight, number of C, O, and N atoms, O/C, and total number of products identified by HPLC-ESI-MS analysis of aerosol collected from O_3 and NO_3 (O_3 + NO_2 + NO_3) oxidation of each monoterpene studied. The difference in average value for each parameter (Δ_{avg}) from each oxidation scheme was also tabulated for each monoterpene.

	α-pinene			**β-pinene**		
	O_3	NO_3	Δ_{avg}	O_3	NO_3	Δ_{avg}
MW_{avg}	237.6 $\pm$ 86.9	233.9 $\pm$ 81.0	-3.7	212.0 $\pm$ 88.9	249.3 $\pm$ 104.3	37.3
C_{avg}	13.8 $\pm$ 5.4	13.2 $\pm$ 5.0	-0.6	12.0 $\pm$ 4.5	12.7$\pm$ 4.7	0.7
O_{avg}	2.9 $\pm$ 1.6	3.1 $\pm$ 1.7	0.2	2.9 $\pm$ 2.1	4.2 $\pm$ 2.6	1.3
N_{avg}	0.29 $\pm$ 0.53	0.40 $\pm$ 0.58	0.11	0.14 $\pm$ 0.36	0.74 $\pm$ 0.73	0.60
O/C	0.22 $\pm$ 0.11	0.25 $\pm$ 0.14	0.03	0.23 $\pm$ 0.12	0.32 $\pm$ 0.16	0.09
# ID'd	28	43	15	29	66	37
	Δ-carene			**limonene**		
MW_{avg}	191.7 $\pm$ 56.9	232.1 $\pm$ 111.5	40.4	216.9 $\pm$ 81.2	306.5 $\pm$ 128.6	89.6
C_{avg}	11.0 $\pm$ 3.1	12.4 $\pm$ 4.7	1.4	12.3 $\pm$ 4.2	14.7 $\pm$ 4.8	2.4
O_{avg}	2.4 $\pm$ 1.2	3.6 $\pm$ 3.0	1.2	2.9 $\pm$ 1.8	5.9 $\pm$ 4.0	3.0
N_{avg}	0.09 $\pm$ 0.30	0.41 $\pm$ 0.67	0.32	0.18 $\pm$ 0.46	0.94 $\pm$ 1.06	0.76
O/C	0.22 $\pm$0.11	0.27 $\pm$ 0.14	0.05	0.23 $\pm$ 0.13	0.39 $\pm$ 0.23	0.16
# ID'd	32	70	38	34	85	51